

# Supporting Information

Oganov et al. 10.1073/pnas.0910335107

## SI Text

Figs. 1–3 show the structures of the found phases of calcium under pressure, whose details are given in Table 1. Table 2 summarizes the pressure-induced transitions of Ca, Sr, and Ba. Experimental results are compared with the present theoretical predictions. The similarity between the phase diagram of Sr and the predicted for Ca is clear.

Fig. 4 describes the density of states (DOS) of Ca at 50 GPa in both sc and  $\beta$ -tin phases. It is clear from the figure that a Peierls transition drives the distortion of the former, as it can be deduced from the energy-lowering opening of a (pseudo)gap at the Fermi level in the  $\beta$ -tin phase.

Fig. 5 displays the phonon spectrum of Ca in the  $\beta$ -tin phase at 60 GPa. The area of each circle is proportional to the partial contribution to the electron-phonon coupling

$$\lambda_{q\nu} \propto \gamma_{q\nu} / \omega_{q\nu}^2 \quad [\text{S1}]$$

where  $\gamma_{q\nu}$  is the linewidth of the mode  $\nu$  at point  $\mathbf{q}$  associated to the electron–phonon interaction and  $\omega_{q\nu}$  its frequency. The Eliashberg function depicted in the right panel, together with the phonon density of states (PDOS), is calculated as

$$\alpha^2 F(\omega) = \frac{1}{2\pi N(0)} \sum_{q\nu} \frac{\gamma_{q\nu}}{\omega_{q\nu}} \delta(\omega - \omega_{q\nu}). \quad [\text{S2}]$$

The mode with largest contribution corresponds to a softening optical mode. This is clear from the large circles of the figure and the lack of correspondence between the Eliashberg function and the PDOS. This mode is the transverse, unstable and very anharmonic mode at M found in sc-Ca. Such correspondence can be deduced from the eigenvectors of the dynamical matrices. Table 3 summarizes the results obtained for the electron–phonon parameters that enter into McMillan equation for different pressures and phases. The logarithmic average frequency is calculated as

$$\omega_{\log} = \exp\left(\frac{2}{\lambda} \int_0^\infty d\omega \frac{\alpha^2 F(\omega)}{\omega} \ln \omega\right) \quad [\text{S3}]$$

where

$$\lambda = 2 \int_0^\infty d\omega \frac{\alpha^2 F(\omega)}{\omega} \quad [\text{S4}]$$

is the electron–phonon coupling constant.

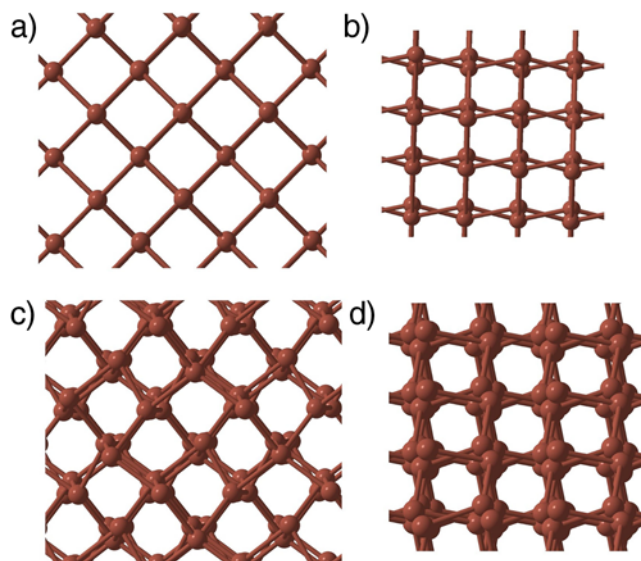


**Fig. S1.** C2/c-12 (Sr-IV) structure in two views (a, b and c, d, respectively) at 50 GPa and 100 GPa (from left to right). At 50 GPa the structure collapses into  $\beta$ -tin structure from which it appears as a result of a symmetry lowering second-order phase transition at 71 GPa. This figure shows a close relationship between these two structures.





**Table S1. Structural parameters at 130 GPa of some of the structures studied**

Wyckoff position	x	y	z
$\beta$ -tin phase ( $I4_1/amd-4$ ), space group origin 2 $a = b = 4.3447$ , $c = 2.4286$ (Å)			
Ca 4b	0.00000	0.25000	0.37500
Sr-IV type phase ( $C2/c-12$ ) $a = 6.2387$ , $b = 6.2205$ , $c = 4.4055$ (Å), $\beta = 130.35^\circ$			
Ca1 4e	0.00000	0.80441	0.25000
Ca2 8f	0.78656	0.59057	0.42230
$P4_32_12-8$ (Ishikawa's phase IV) $a = b = 3.1219$ , $c = 9.0619$ (Å)			
Ca 8b	0.82148	0.48884	0.09360
$Pnma-4$ $a = 4.3924$ , $b = 3.3952$ , $c = 2.8968$ (Å)			
Ca 4c	0.67192	0.75000	0.60785
$C2/m-32$ (host-guest) $a = 9.3272$ , $b = 7.9100$ , $c = 4.2588$ (Å), $\beta = 111.42^\circ$			
Ca1 4e	0.25000	0.25000	0.00000
Ca2 4g	0.00000	0.25032	0.00000
Ca3 4h	0.00000	0.35141	0.50000
Ca4 4i	0.55122	0.50000	0.79665
Ca5 8j	0.66691	0.64776	0.49473
Ca6 4i	0.78483	0.50000	0.20689
Ca7 4i	0.88316	0.50000	0.79922
$I4/mcm-32$ (host-guest) $a = b = 5.7013$ , $c = 9.7242$ (Å)			
Ca1 16l	0.14875	0.35125	0.16698
Ca2 8h	0.85577	0.35577	0.00000
Ca3 4 <sup>a</sup>	0.50000	0.50000	0.75000
Ca4 4c	0.50000	0.50000	0.00000
$C2/c-32$ (host-guest) $a = 6.4352$ , $b = 5.5812$ , $c = 8.3430$ (Å), $\beta = 102.93^\circ$			
Ca1 8f	0.67849	0.39980	0.78435
Ca2 8f	0.62086	0.75378	0.87638
Ca3 8f	0.52341	0.10576	0.61580
Ca4 8f	0.84411	0.90096	0.44914
$C2/c-24$ $a = 7.6867$ , $b = 4.4218$ , $c = 8.3884$ (Å), $\beta = 114.23^\circ$			
Ca1 8f	0.77472	0.24566	0.80848
Ca2 8f	0.02764	0.82753	0.90171
Ca3 8f	0.89154	0.33840	0.59753
$Cmca-8$ (Ishikawa's phase V) $a = 4.3693$ , $b = 4.5658$ , $c = 4.3875$ (Å)			
Ca 8f	0.00000	0.65701	0.30797
$Cmca-16$ $a = 4.3221$ , $b = 7.9473$ , $c = 5.2744$ (Å)			
Ca1 8f	0.00000	0.7880	0.0533
Ca2 8f	0.00000	0.0235	0.2940

The unit cell parameters are given in Å. The Wyckoff orbits are indicated together with the position in the cell of one of its representatives.

**Table S2. Summary of high-pressure behavior of Ca, Sr, and Ba**

	fcc	bcc	sc derivative structures:				Host-guest	hcp
			$I4_1/amd$ , ( $\beta$ -tin)	$C2/c-12$ (Sr-IV)	$P4_32_12-8$	$Pnma-4$	$C2/m-32$	
Ca	0–19.5 GPa (0–8 GPa)	19.5–32 GPa (8–33 GPa)	32–113 GPa (sc) (33–71 GPa)	(71–89 GPa)	113–139 GPa (89–116 GPa)	?	>139 GPa (134–564 GPa)	?
Sr	0–3.5 GPa	3.5–26 GPa	26–35 GPa	35–26.3 GPa			>46.3 GPa	?
Ba		0–5.5 GPa*					12.6–45 GPa	>45 GPa

For Ca the theoretical results presented here are given in parenthesis.

\*at 5.5–12.6 GPa Ba adopts the hcp structure (reentrant above 45 GPa)

**Table S3. Summary of the calculated magnitudes entering McMillan equation in the different phases**

	Pressure (GPa)	$\omega_{\log}(\text{K})$	$\lambda$	Tc(K)
<i>I4<sub>1</sub>/amd-4</i>	60	188.7	0.67	5.8
<i>C2/c-12 (Sr-IV)</i>	80	80.4	1.33	8.1
<i>P4<sub>3</sub>2<sub>1</sub>-8</i>	110	140.7	2.06	20.6
<i>Pnma-4</i>	120	333.0	0.96	21.9
<i>Pnma-4</i>	130	348.5	0.98	23.5